Comparison of Two Modeling Approaches for Thin-Plate Penetration Simulation

Norman F. Knight, Jr.
Veridian-MRJ, Yorktown, VA, USA
303 Heaven's Way
Yorktown, VA 23693-2619
Tel.: (757) 867-6394
Fax: (757) 867-6394
e-mail: knight@mrj.com

Navin Jaunky
Eagle Aeronautics, Newport News, VA, USA

Robin E. Lawson
FDC/NYMA, Hampton, VA, USA

Damodar R. Ambur
NASA Langley Research Center, Hampton, VA, USA

Abbreviations:

CTSF	Computed time step factor
EE	Element erosion
FAA	Federal Aviation Administration
NASA	National Aeronautics and Space Administration
SIPF	Sliding interface penalty factor
TNWF	Tied nodes with failure

Keywords:
Contact, impact, penetration, tied-nodes-with-failure, element erosion

ABSTRACT

Modeling and simulation requirements for uncontained engine debris impact on fuselage skins are described and assessed using the tied-nodes-with-failure (TNWF) approach and the element-erosion (EE) approach for penetration simulation. The TNWF approach is based on coincident nodes generated in selected regions of the target plate that are tied together using a constraint relation and the target plate is modeled with shell elements. The EE approach is based on eliminating or removing of an element once some criterion is reached.

INTRODUCTION

Prediction of the elasto-plastic, large-deformation, transient dynamic behavior involving impact of multiple deformable bodies continues to provide new insights into the response of complex structural systems subjected to extreme loading conditions. One such application involves simulating the response of a fuselage skin when impacted by uncontained aircraft turbine-engine debris. Two potential hazards involving the turbine-engine debris are the subject of ongoing research efforts. One event involves containing failed engine debris within the engine housing - contained failure. The other event involves the potential impact of failed engine debris on other parts of the aircraft - uncontained failure. Examples of research in these areas include Ambur (1999), Knight (1999), Lawson (1999), Ollivier (1999), Olmi (1999), Sarkar (1995), and Shockey (1997). Developing accurate finite element models and analysis strategies to simulate these events has the potential of significantly improving the design, reliability, and safety of engines and primary aircraft structures, especially for commercial transport applications.

The objective of this paper is to compare two approaches for simulating penetration of thin aluminum plates impacted by titanium fragments using the LS-DYNA nonlinear transient dynamic finite element code (Hallquist, 1997). These simulations are related to the impact and penetration scenario that would result from uncontained engine debris striking a fuselage skin. One configuration, studied previously by Shockey (1997), is referred to herein as the SRI configuration. Another configuration, studied by Ambur (1999), is referred to herein as the NASA configuration. Both test facilities have similar features, capabilities, and objectives. This investigation assesses the different penetration modeling approaches for this type of problem. Selected parametric studies are performed for the NASA configuration to determine a threshold initial velocity for penetration.

APPROACH

The basic SRI configuration considered in this study has been defined by Shockey (1997). It is studied to provide some level of verification for the present simulations using LS-DYNA by comparing with the limited test results given by Shockey (1997). Numerous tests were performed by SRI along with selected DYNA3D finite element simulations. The SRI tests use a small 0.06 lb titanium fragment with truncated corners and a 6-in. square aluminum target barrier with a 0.040-in. thickness. The initial speed of the impact fragment was 312 fps for the complete penetration simulation.

The basic NASA configuration considered in this study has been defined by Ambur (1999). The NASA configuration uses a 0.654-lb titanium rectangular-shaped fragment and a 20-in. square aluminum target barrier with a 0.040-in. thickness. The initial speed of the impact fragment was varied in the simulation to determine the threshold velocity for the complete penetration. Only a single test has been run and simulation results for that case are presented.

Modeling for Penetration

Penetration of the target plate can be simulated in at least two ways depending on the modeling approach used for the target plate itself. One way is the tied-nodes-with-failure (TNWF) approach, and the other way is the element-erosion (EE) approach. Using the TNWF approach, coincident nodes are generated in selected regions and then tied together with a constraint relation. In LS-DYNA, these tied nodes remain together until the volume-weighted effective plastic strain, averaged over all elements connected to the coincident nodes in a given constraint, exceeds a specified value. Once this value is exceeded, all nodes associated with that constraint are released to simulate the initiation of a crack, fracture or penetration. Using the EE approach, the finite element model is generated in the standard manner without requiring duplicate or coincident nodes. Once the effective plastic strain in an element reaches a specified critical value or the critical time step size for a given element becomes smaller than a specified minimum value, the element is removed from the computations. Element erosion is the process used to eliminate elements during the computation that no longer contribute to the overall response determination. Eroding elements are elements that are destroyed during the course of the computation because of very high strains. While some mass is lost in the EE approach, conservation of momentum is insured.

Modeling

The finite element modeling strategy for the TNWF penetration modeling approach used herein is essentially the same as that used by Shockey (1997). For the EE penetration modeling approach, both shell elements and solid elements were used to model the target plate wherein the mesh generation process does not need to include duplicate or coincident nodes. In all cases, the simulation model involves three components: impactor, test fixture frame, and target plate. Finite element refinement studies are performed wherein different levels of mesh refinement are used for the barrier target region. Refinement in the barrier target plate region naturally extends into the test fixture frame in order to have compatible meshes. In the present study, the sliding interface with friction and separation approach (Interface Type 3) is used to model the impact event between the impactor and the barrier target plate. The bounding surface of three-dimensional impactor is treated as the slave surface, and the target plate is treated as the master surface. Contact modeling issues have been discussed by Reid (1998), and the need for evaluating modeling techniques and code features advocated.

Impactor. The impactor is modeled using 8-node solid elements with an elastic-plastic strain-hardening material model (Material Type 3) and given an initial speed in the x-direction. The impactor is initially positioned slightly away from the target, and its orientation (pitch and roll) is specified. The impactor is made of titanium. The spatial discretization of the impactor is held constant regardless of the mesh refinement used for the other components.

Test Fixture Frame. The test fixture frame is also modeled using 8-node solid elements with an elastic-plastic strain-hardening material model (Material Type 3). The frame has a lower part and an upper part that are assembled together to clamp down on the target plate. For the SRI configuration, the test fixture frame parts are made of titanium. The frame for the NASA configuration is of similar construction except that it is larger and made from steel. The spatial discretization of the test frame through its thickness involves two 8-node solid elements. The spatial discretization in its plane is determined by the spatial discretization used for the target plate. Boundary conditions are imposed on the nodes in the test frame model to prevent any motion (i.e., rigid test frame).

Target Plate. The target plate is modeled using either 4-node Belytschko-Lin-Tsay shell elements or 8-node solid elements with an elastic-plastic strain-hardening material model. In the TNWF approach, an ultimate failure strain of 0.20 in./in. is used as the constraint value to

release any tied nodes once the element strain reaches this level. In the EE approach, this value is also used to eliminate (or erode) elements once the element strain level reaches 0.20 in./in. The time step size for element deletion is 0.07μsec - roughly one order of magnitude smaller than the computed critical time step size for any element in the simulation. In the TNWF approach, the target plate uses Material Type 3; however, in the EE approach with shell elements, Material Type 24 is used.

In the TNWF approach, the finite element modeling strategy used for the target plate involves three separate regions (see Figure 1). First is the boundary region restrained by the test fixture, then there is an outer region which is in the test area and assumed not to be penetrated by the impactor, and finally there is the inner region of the test area for which penetration may occur. Elements in the boundary region of the target plate overlap elements in the test fixture frame parts. The finite element models of the upper and lower test frame parts and the target plate are then joined together as in the test configuration. The test area of the target is modeled by two regions: an outer region that extends from the frame boundary to the inner region. The inner region is the area of probable impact and possible penetration. This inner region of the target plate is called the "shell-break" area. In this area, elements are individually created with their own independent nodes. Coincident nodes are then identified and tied together until the average volume-weighted plastic strain exceeds a specified value. Spatial discretization in the shell-break area determines the element distribution throughout the target plate for the most part.

In the EE approach, the finite element modeling strategy for the target plate is the traditional modeling approach with mesh grading near the impact site but does not require any coincident nodes. Two idealizations of the target plate were considered: 4-node shell elements and 8-node solid elements. The solid element approach allows material to be eroded away more gradually than the shell element model as the impactor penetrates the target plate because of the through-the-thickness modeling.

NUMERICAL RESULTS AND DISCUSSION

Penetration of a thin aluminum plate mounted in a near-rigid frame and impacted by a titanium impactor is considered in this study. The response of the structure is studied by examining the normal displacement and normal velocity as well as the energies and contact force. The results generated are obtained using LS-DYNA Version 940.

Results for the SRI Penetration Case using TNWF

This case has an initial impactor velocity of 312 fps and an orientation given by a -9.3° pitch angle and a -9.5° roll angle. This velocity exceeds the threshold value for penetration, however, it does correspond to the condition used in the SRI simulation. Four different meshes were considered – Mesh 1 being the coarsest mesh and Mesh 4 being the most refined.

The deformed geometry for Mesh 4 at complete penetration is shown in Figure 2a. From the TNWF model, a damage area corresponding to the large hole "punched" by the impactor is clearly evident as are additional small fragments generated by the "tearing" of this hole. The tearing of the tied nodes occurs once the volume-weighted plastic strain reaches a value of 0.2 in./in. A close-up view of the impact site is shown in Figure 2b with contours of the plastic strain. A large region of plastic strain is predicted in the vicinity of the impact, and the overall transient dynamic response is somewhat localized.

A comparison of the axial (x-direction) velocity component of Node 675 at the center of the impactor for the finite element models considered is given in Figure 3. The Mesh 1

simulation indicated that at approximately 0.4 msec, the impactor has clearly rebounded after impact. The more refined models predict penetration of the plate. The residual speed of the impactor (i.e., velocity in the x-direction after penetrating the plate) for Mesh 4 is higher than for Mesh 2 by nearly a factor of two. The residual speed of the impactor is 173 fps from Mesh 4 which is approximately 14% lower than the test result of 203 fps from Test 6 given by Shockey (1997).

The effect of the sliding interface penalty factor (SIPF) on predicting the response of the plate during the penetration case is shown in Figure 4 in terms of the total energy as a function of time. Using Mesh 3, the penetration simulation is attempted using various SIPF values. For values of 1.0, 0.1 and 0.01, the initial portion of the simulation appears correct, and then the total energy suddenly increased. Associated with each jump in total energy shown in Figure 4 are out-of-range values for the velocities. These values thereby caused the kinetic energy to grow without bound, and hence the total energy grew without bound until the simulation stops. When SIPF equals 0.001, the impactor penetrated the target by about 7% of its length before any "tearing" of the target elements occurred (i.e., "no damage" penetration). This appreciable "no-damage" initial penetration led to a "soft" impact where the impactor traveled 1.79 inches after 1 msec of simulation time. The residual velocity of the impactor after penetration is about 89 fps, and the total energy is below the initial energy for almost the entire simulation. The maximum value of the ratio of the sliding interface energy to initial energy is about 0.1%. "No-damage" penetration tends to occur when the ratio of the maximum sliding interface energy to initial energy ratio is very small. In such cases, the SIPF value is normally too small for the impact simulation considered and needs to be increased. When SIPF equals 0.006, the impactor traveled 2.4 inches after 1 msec of simulation time. The residual velocity of the impactor after penetration is about 192 fps when SIPF equals 0.006 or about twice the value predicted when SIPF equals 0.001. At approximately 0.56 msec, the impactor has completely penetrated and passed through the plate. The slight increase in total energy as the sliding interface energy goes to zero is evident in Figure 4.

Results for the SRI Penetration Case using EE

In the EE modeling approach for the SRI case, both the target plate and impactor are modeled using three-dimensional 8-node solid elements. The eroding surface-to-surface approach (Interface Type 14) is used to model the contact event between the impactor and the barrier target plate. Once the effective plastic strain in an element reaches 0.2 in./in. or when the critical time step size for the element reaches 0.07μsec, the element is removed (or "eroded") from the computations.

Three different in-plane mesh discretizations are considered based on the in-plane element edge length. Meshes 1 and 2 have the same uniform in-plane discretizations as their counterparts in the TNWF approach. Mesh 3 has a non-uniform in-plane discretization with refinement near the impact site. Four different through-the-thickness mesh discretizations are considered for the target. In the notation Mesh *i:j*, the "*i*" denotes the in-plane spatial discretization mesh and the "*j*" denotes the number of elements through the thickness. The penetration simulation performed in this study has an initial impactor velocity of 312 fps and an orientation given by a -9.3° pitch angle and a -9.5° roll angle, identical to the TNWF penetration case.

The deformed geometry with the plastic strain distribution for Mesh 3:4 after penetration are shown in Figure 5. Complete penetration of the target plate by the impactor is evident. The overall transient dynamic response is much more localized than the damage predicted using the TNWF approach (compare Figure 5 with Figure 2b). Petaling of the target plate is also clearly visible. At approximately t = 0.17 msec, elements begin to "fail" and are eliminated

from the simulation. By t = 0.35 msec, 182 elements have been removed. This corresponds to a hole size of approximately 0.267 in. × 1.125 in. × 0.040 in. The hole size predicted using the EE approach is approximately 26% smaller than that predicted in the TNWF approach. Although Mesh 3 using the EE approach is a coarser mesh than Mesh 4 using the TNWF approach, the three dimensional modeling of through-the-thickness failures helps to localize the failure near the impact site. That is, the solid elements erode in the thickness direction while the shell elements account for through-the-thickness effects in the kinematics.

A comparison of the total energy for the finite element models considered is given in Figure 6. Mesh 1:2 results exhibit similar trends as those predicted in the TNWF Mesh 1 case (i.e., rebound behavior). As in the TNWF approach, the other meshes have a different behavior. As Mesh 2 is refined through the thickness, the responses appear to "converge," yet still indicate a large energy loss overall. Mesh 3:3 and 3:4 mirror each other in their response predictions. Notice that at the approximate time the elements begin to erode ($t \geq$0.17 msec), the total energy loss significantly increases (see Figure 6). Although, with each in-plane mesh refinement, the total energy loss decreases. In the EE approach, elements "erode" once the strain level reaches 0.2 in./in. When an element is "eroded", its internal energy as well as its kinetic energy is lost. The mass loss is redistributed so that momentum is conserved (Hallquist, 1997). As a result, significant energy loss may occur for the EE cases. The TNWF cases "break off" elements but do not eliminate them, hence their energies are still included in the energy calculation. The results obtained for Mesh 3:3 and 3:4 indicate less of an energy loss. Mesh 3:4 is considered as the "reference" solution in the EE simulations. These results also indicate that, for this case, three elements throughout the thickness of the target plate is sufficient. However, the bending behavior is very localized and when substantial bending occurs, the number of elements through the thickness will need to be increased.

As in the TNWF studies, the effect of the sliding interface penalty factor (SIPF) on predicting the response of the plate during the penetration case is studied. Using Mesh 2:2, the penetration simulation is attempted using two SIPF values; 0.0025 and 0.005. For SIPF of 0.0025, the impactor penetrated the target barrier plate with no damage resulting to the plate (i.e., the simulation was too "soft"). By increasing the SIPF to 0.005, the simulation appears correct with elements of the plate reaching the maximum value of the plastic strain and element erosion occurs.

Results for the NASA Configuration using TNWF and EE

The NASA configuration is similar to the SRI configuration in general. However, the unsupported test region of the target plate and the impactor are both much larger. The simulations performed contributed to the overall design and verification of the NASA gas-gun facility. Parametric studies were performed prior to any testing to determine the threshold velocity for the impactor "just" to penetrate the target plate.

The threshold velocity for the impactor with zero pitch, roll and yaw angles obtained using the TNWF approach (Mesh TNWF-1) is 250 fps, while that obtained using the EE approach (Mesh EE-1) is 200 fps. This lower threshold velocity is due to Mesh EE-1 being a more refined mesh along the impactor width direction compared to Mesh TNWF-1. Hence Mesh TNWF-1 is a slightly stiffer model compared to Mesh EE-1. The simulation was carried out with SIPF = 1.0E-03, CTSF = 0.6, and the value of Max (SIE/TE) obtained was 3.5%. The rebound velocity obtained using either penetration modeling approach is approximately the same; that is ≈40 fps with zero pitch, roll, and yaw angle. This is considered to be nearly a converged value.

A comparison of the fringe plot of the effective plastic strain of the target for the TNWF approach and the EE approach is shown in Figure 7 at their respective termination time. The effective plastic strain zone for Mesh TNWF-1 is different from that of Mesh EE-1. The partial perforation of the target plate by the impactor can be seen in Mesh TNWF-1 model. In the Mesh EE-1 model, the impact event has produced two vertical cracks along the target plate. The damage obtained using Mesh EE-1 model is also symmetric.

A test was conducted with an impactor axial velocity of 450 fps (more than twice the threshold value), and the impactor penetrated the aluminum target. On examining the damaged target, it was observed that the impactor made contact with the target at 1.19 inches below the center of the target and the roll angle of the impactor was 4.76°. The impactor had an initial roll angle of 5°. This observation suggests that the impactor had a different pitch angle. The exact pitch angle is difficult to assess since some test conditions were unknown; however, an estimate of the pitch angle is 4.7°. A photograph of the region around the impact site of the test target is shown in Figure 8(a). The impactor has punched a big hole in the target, resulting in petaling and longitudinal cracks.

Various simulations were performed using different roll and pitch angles and different impactor initial speeds (Ambur, 1999). Simulation results were obtained using EE approach and Mesh EE-2. This model has a larger area with a refined mesh than Mesh EE-1. The values used for SIPF and CTSF are 0.001 and 0.6, respectively. The termination time was 1.0 msec. The maximum value of the sliding interface energy to total energy is 0.01%, and the residual axial velocity was 40 fps. A close-up view of the effective plastic strain distribution in the target plate, with the impactor removed for clarity, is shown in Figure 8(b). The effective plastic strain is more localized around the hole. The formation of tears and petaling can also be seen.

SUMMARY

A comparative study of two modeling approaches for thin-plate penetration problems has been performed. One approach is the tied-nodes-with-failure approach which requires coincident nodes and a constraint. Here the thin plate is modeled using shell elements. The other approach is the element erosion approach that erodes or eliminates elements from the model once a specified limit is reached. Here the thin plate is modeled with either shell elements or solid elements. Both approaches offer advantages. TNWF approach requires extra modeling effort to generate coincident nodes and constraint equations; but it does conserved mass. EE approach uses the standard modeling approach; but while is does conserve momentum, it does not conserve mass. Shell element models using EE are computationally faster and capture the bending behavior well. Solid element models with EE are generally very large computational problems but can capture the through the thickness damage of the plate. For thin isotropic plates, shell models are recommended. For composite laminated plates, solid models need to be examined to study the progressive damage response. The results presented indicate prediction of local damage details requires very refined finite element models.

ACKNOWLEDGMENTS

The work of the first two authors was supported by NASA Cooperative Agreement NCC-1-284 before they left ODU. The work of the third author was supported by the NASA Graduate Student Researcher Program Grant No. NGT-1-52173 and by a Virginia Space Grant Fellowship before she left ODU. This support is gratefully acknowledged.

REFERENCES

AMBUR, D.R., JAUNKY, N., LAWSON, R.E., KNIGHT, N.F., JR., and LYLE, K.H. (1999). "A Gas-Actuated Projectile Launcher for High-Energy Impact Testing of Structures," AIAA Paper No. 99-1385.

HALLQUIST, J.O. (1997). *LS-DYNA User's Manual – Version 940*, Livermore Software Technology Corporation.

KNIGHT, N. F., JR., JAUNKY, N., LAWSON, R.E., and AMBUR, D.R. (1999). "Modeling and Simulation for Uncontained Engine Debris Impact on Fuselage Skins using LS-DYNA3D," AIAA Paper No. 99-1573.

LAWSON, R.E. (1999) *LS-DYNA3D Modeling and Simulation for Uncontained Engine Debris Impact on Fuselage Skins*, Master's Thesis, Department of Aerospace Engineering, Old Dominion University, Norfolk, VA.

OLLIVIER, ANDRE (1999). "Structure Simulation and Blade Design of an Aircraft Engine," *1999 MSC Worldwide Aerospace Conference Proceedings - Volume 1*.

OLMI, FRANCO and DINIZ DO NASCIMENTO, KENNEDY (1999). "Small Debris Impact Simulation Using MSC/DYTRAN," *1999 MSC Worldwide Aerospace Conference Proceedings - Volume 1*.

REID, J.D. (1998). "Admissible Modeling Errors or Modeling Simplifications?," *Finite Elements in Analysis and Design*, Vol. 29, pp. 49-63.

SARKAR, S. and ATLURI, S.N. (1995). "Impact Analysis of Rotor Fragments on Aircraft Engine Containment Structures," *Structural Integrity in Aging Aircraft*, C. I. Chang and C. T. Sun (editors), ASME, AD-Vol. 47, pp. 87-97.

SHOCKEY, D.A., GIOVANOLA, J.H., SIMONS, J.W., ERLICH, D.C., KLOPP, R.W., and SKAGGS, S.R. (1997). *Advanced Armor Technology: Application Potential for Engine Fragment Barriers for Commercial Aircraft*, Federal Aviation Administration Report No. DOT/FAA/AR-97/53.

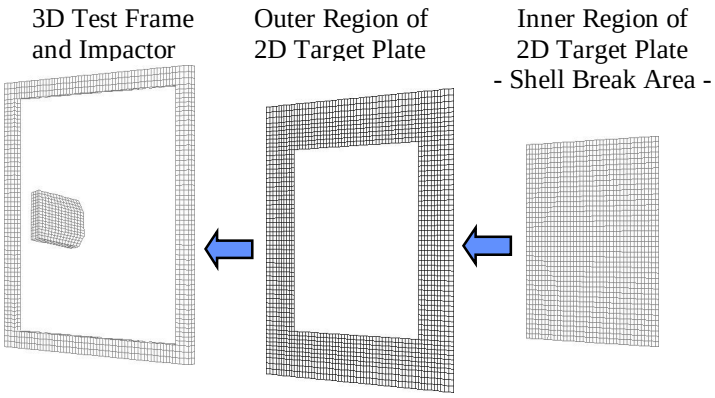

Figure 1. Finite element model strategy for the TNWF approach.

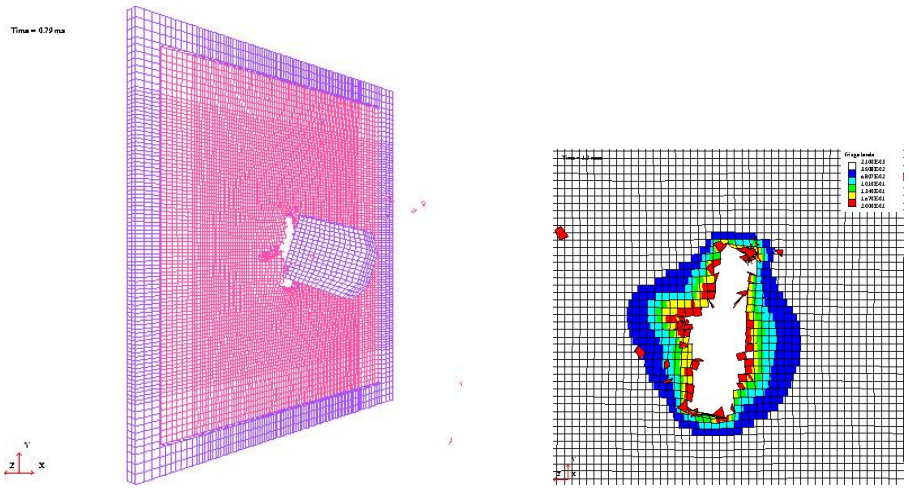

(a) Deformed geometry plot. (b) Close-up of plastic strain distribution.

Figure 2. Mesh 4 results after complete penetration for the TNWF approach.

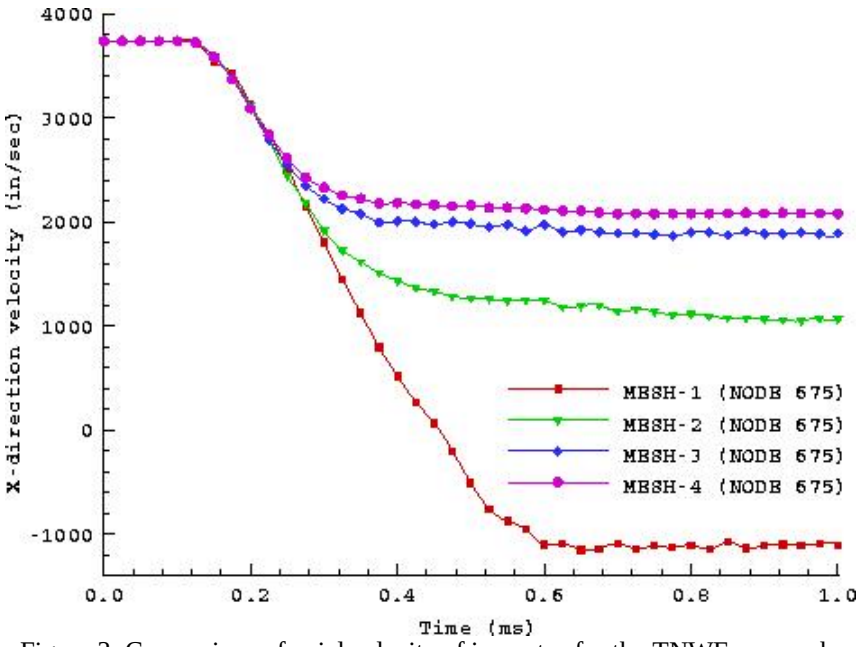

Figure 3. Comparison of axial velocity of impactor for the TNWF approach.

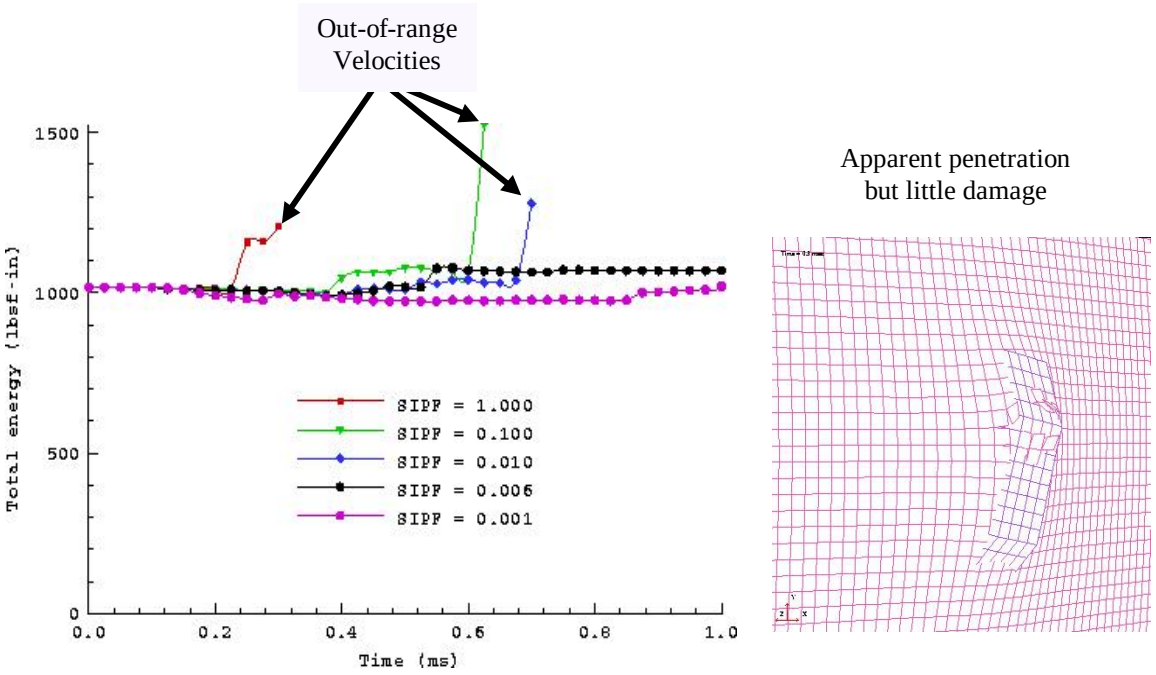

Figure 4. Effect of SIPF on total energy for Mesh 3 with the TNWF approach.

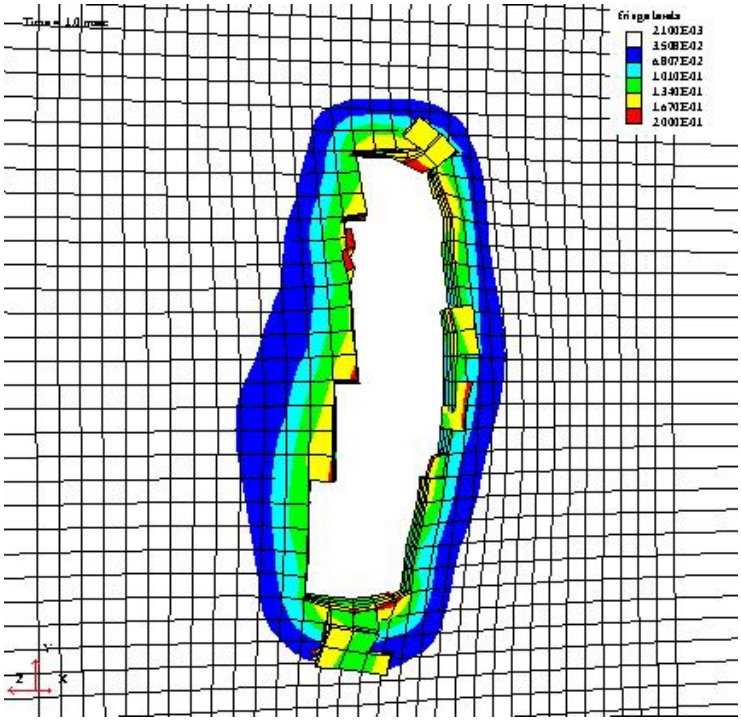

Figure 5. Close-up view of plastic strain distribution near the impact site after complete penetration (EE approach, Mesh 3:4).

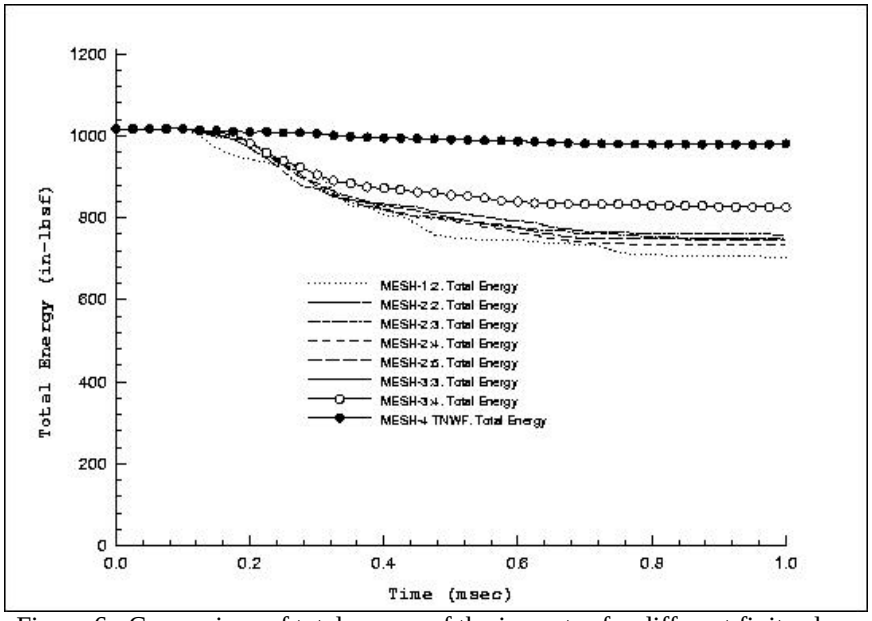

Figure 6. Comparison of total energy of the impactor for different finite element models of the target plate using the EE approach.

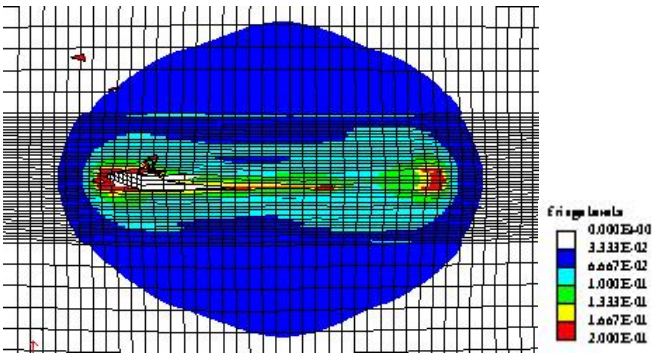

(a) Results for Mesh TNWF-1 at threshold velocity.

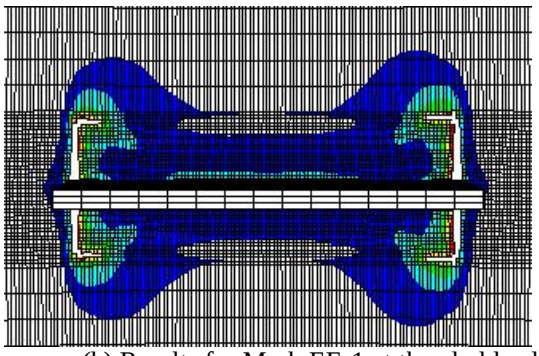

(b) Results for Mesh EE-1 at threshold velocity.

Figure 7. Close-up view of the effective plastic strain distribution.

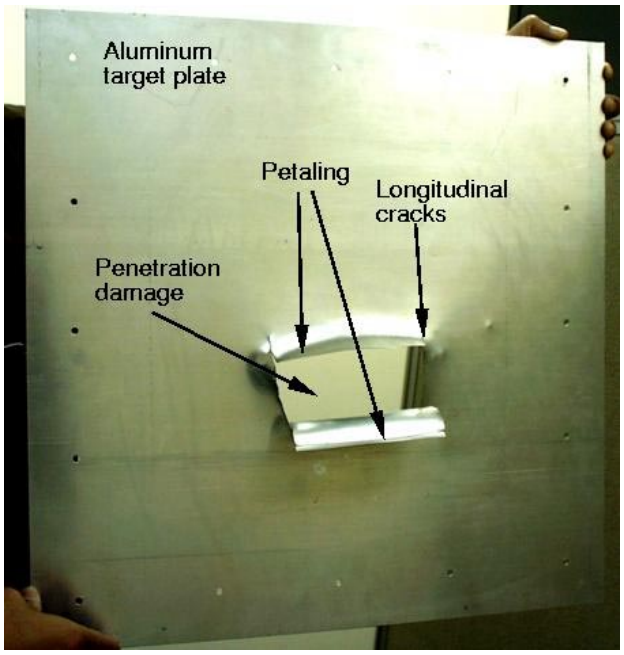

(a) Photograph of test specimen after impact and penetration.

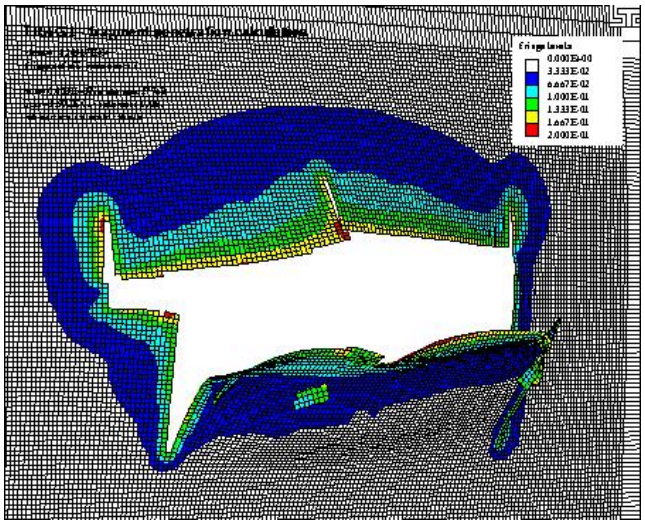

(b) Close-up view of effective plastic strain distribution on Mesh EE-2.

Figure 8. Comparison of damaged aluminum target plate with simulation results for initial impactor speed of 450 fps.